Bragg gratings in bulk media
by Andrew John Heltborg

A thesis submitted in partial fulfillment of the requirements for the degree of Master of Science in Electrical Engineering
Montana State University

Abstract:
This thesis investigates the creation of distributed Bragg reflectors in bulk optical materials for lasers and sensors. The underlying hypothesis of this thesis is the supposition that crystal growth techniques can result in the formation of precisely defined periodic variations in the refractive index of a crystalline or glassy solid. Crystals of CTH: YAG and Tm:YAG were fabricated utilizing various growth techniques. The crystals were characterized using SEM cathodoluminescence (CL) imaging and spectra, optical diffraction techniques, and mid-infrared transmission and reflection measurements. The CTH:YAG crystals showed a periodic variation in dopant concentrations (striae) using the CL imaging. The CL spectra were used to determine that most of the striae were due to thulium (Tm3+) with some contribution from chromium (Cr3+) and minimal contribution from holmium (Ho3+). The TmiYAG crystals showed no striae with any of the measurement techniques. Optical diffraction was used to measure the pitch of the Bragg gratings to verify the SEM CL data. The search for Bragg reflections from the crystals is still ongoing. This data proves that the growth techniques are viable methods to produce Bragg gratings in bulk optical material.

BRAGG GRATINGS IN BULK MEDIA

by

Andrew John Heltborg

A thesis submitted in partial fulfillment
of the requirements for the degree

of

Master of Science

in

Electrical Engineering

MONTANA STATE UNIVERSITY
Bozeman, Montana

May 2000

APPROVAL

of a thesis submitted by

Andrew John Heltborg

This thesis has been read by each member of the thesis committee and has been found to be satisfactory regarding content, English usage, format, citations, bibliographic style, and consistency, and is ready for submission to the College of Graduate Studies.

Chris Yakymyshyn
Committee Chair (Signature) April 11, 2000 (Date)

Approved for the Department of Electrical & Computer Engineering

John Hanton
Department Head (Signature) 4-11-00 (Date)

Approved for the College of Graduate Studies

Bruce McLeod
Graduate Dean (Signature) 4-13-00 (Date)

STATEMENT OF PERMISSION TO USE

In presenting this thesis in partial fulfillment of the requirements for a master's degree at Montana State University, I agree that the Library shall make it available to borrowers under the rules of the Library.

If I have indicated my intention to copyright this thesis by including a copyright notice page, copying is allowable only for scholarly purposes, consistent with "fair use" as prescribed in the U.S. Copyright Law. Requests for permission for extended quotation from or reproduction of this thesis in whole or in parts may be granted only by the copyright holder.

Signature Andy Hattery

Date April 11, 2000

TABLE OF CONTENTS

LIST OF TABLES

LIST OF FIGURES

LIST OF FIGURES – CONTINUED

ABSTRACT

This thesis investigates the creation of distributed Bragg reflectors in bulk optical materials for lasers and sensors. The underlying hypothesis of this thesis is the supposition that crystal growth techniques can result in the formation of precisely defined periodic variations in the refractive index of a crystalline or glassy solid. Crystals of CTH:YAG and Tm:YAG were fabricated utilizing various growth techniques. The crystals were characterized using SEM cathodoluminescence (CL) imaging and spectra, optical diffraction techniques, and mid-infrared transmission and reflection measurements. The CTH:YAG crystals showed a periodic variation in dopant concentrations (striae) using the CL imaging. The CL spectra were used to determine that most of the striae were due to thulium (Tm^{3+}) with some contribution from chromium (Cr^{3+}) and minimal contribution from holmium (Ho^{3+}). The Tm:YAG crystals showed no striae with any of the measurement techniques. Optical diffraction was used to measure the pitch of the Bragg gratings to verify the SEM CL data. The search for Bragg reflections from the crystals is still ongoing. This data proves that the growth techniques are viable methods to produce Bragg gratings in bulk optical material.

CHAPTER 1

INTRODUCTION

Electromagnetic wave propagation in periodic layered media exhibits some interesting and useful phenomena. The simplest example of a periodic layered structure consists of alternating layers of two different materials of equal thickness. This layered structure can also be made in a single material that has periodic variations in the complex refractive index. Light experiences Fresnel reflections from dielectric interfaces due to variations in the index of refraction. The light reflected from each individual interface is quite small, but if the phase delay of the reflected light is chosen correctly, each reflection adds constructively. It is possible to achieve extremely high reflectance by increasing the number of interfaces. When this phenomenon occurs with light it is referred to as either a distributed Bragg reflector (DBR) or a distributive feedback (DFB) structure.

Over the past 15 years, there has been great success in placing DFB and DBR structures in optical fibers (Culshaw) and semiconductor lasers (Luo). Fiber Bragg gratings are now commercially available and are used in various applications, including optical filtering for optical telecommunications, laser diode spectral control, and fiber sensors. DFB semiconductor lasers are very stable sources with extremely narrow linewidths that make them ideal for long-haul fiber optic telecommunications.

These structures are now being placed in bulk media. Different methods of creating these structures have been tested for dye laser doped polymeric films (Kogelnik) and with color center lasers in alkali halide crystals (Bjorkland). There have not been any investigations into using the more common and useful inorganic oxide/fluoride laser crystals and glasses. Successfully creating a DFB or DBR laser crystal will greatly simplify the manufacturing process for existing solid state laser systems such as microchip lasers and flashlamp pumped rod lasers. The crystals in these laser systems traditionally have a thin film mirrored coating deposited on opposite ends of the crystal to create a laser cavity, but the coatings are problematic, fragile, and expensive. A DFB structure placed inside the crystal will eliminate the need for mirrored coatings.

A DFB microlaser could have an impact on light sources used in telecommunications, medical display, military, and various other commercial applications. The telecommunications industry is moving towards wavelength division multiplexed (WDM) networks that require very stable, low noise laser sources. As the number of channels increase in WDM networks, the problem becomes more significant and special care must be used to prevent aliasing of the different laser sources. Even if a DFB microlaser was not used, a DBR mirror could be utilized to provide a stable feedback element for controlling the spectrum of diode lasers. A DFB microchip laser could also be advantageous in systems used for remote sensing of airborne contaminants for military field use, or emission

compliance for chemical processing plants that require narrow linewidth, stable, modest power, tunable light sources which are not cost prohibitive.

The medical community requires smaller Q-switched sources for microsurgery. A passively Q-switched DBF microlaser may be mounted on the end of an optical fiber to provide a local source of high peak power pulses in a small, elegant handheld device. By incorporating laser ions in a DFB media lacking a center of symmetry, such as Nd^{3+}:$LiNbO_3$, self-doubling or self-OPO devices can be constructed to make efficient visible light sources for projection displays or optical storage (Yakymyshyn).

Solid state lasers provide several advantages over diode lasers, including the ability to efficiently store optical energy and release it in controlled high peak power pulses, and the ability to generate output beams having exceptionally narrow optical linewidths, a low intensity noise, and a TEM_{00} diffraction limited transverse modal distribution. A successful demonstration of high quality distributed gratings in crystals or glassy materials will enable the creation of these devices.

Optical sensors have seen steady growth in the number of commercially successful applications over the past ten years (Dakin and Udd). Two of the most common barriers limiting the introduction of new optical sensors are sensor system cost and the sensor's ability to handle extremely harsh environments. Optical fiber Bragg gratings, for example, have difficulty competing with other technologies because of the costly need to couple light into single mode fiber. If DBR structures can be placed in bulk media, then bulk optical elements become feasible as sensor

elements in which the measurand is spectrally encoded by the reflectivity of the Bragg grating. Because of the use of a bulk material, multi-mode fiber and inexpensive light sources can be used as part of the sensor system, thereby lowering system cost. The sensing element can be a passive filter/reflector or an active laser whose lasing characteristics are modified by the environment. In addition, bulk monoliths can be extremely robust with proper material selection, permitting sensor use in traditionally untenable application areas such as metal foundries, down-hole oil and gas wells, jet engine and rocket engine manifolds, and radioactive waste containment vessels (Yakymyshyn).

The underlying hypothesis of this paper is the supposition that crystal growth techniques can result in the formation of precisely defined periodic variations in the refractive index in a crystalline or glassy monolith. These Bragg gratings will be characterized using scanning electron microscope cathodoluminescence (SEM CL) imaging and spectra, and SEM X-ray analysis and imaging. Optical diffraction will also be used to measure the pitch of the gratings to verify the SEM data. The final stage of this thesis will be to find and characterize any Bragg reflections.

CHAPTER 2

THEORY

Coupled Mode Theory

As mentioned before, distributed Bragg reflectors can have extremely high reflectance for a large number of interfaces. Because stringent phase requirements need to be met for the individual reflections to add, Bragg gratings are spectrally selective. The reflectance of a Bragg grating is typically solved using coupled mode theory, which is based on the assumption that the mode fields of an unperturbed waveguide remain relatively unchanged in the presence of weak perturbations.

The application of coupled mode theory (Yeh) assumes that the change in index of refraction is sinusoidal in nature. The index of refraction can be written as either

$$n(x) = n_0 + n_1 \cos(Kx), \tag{2-1}$$

or

$$n(x) = n_0 + n_1 \sin(Kx), \tag{2-2}$$

where n_0 is the average index of refraction of the material, n_1 is the depth of the modulation of the index, and K is the grating wave vector. K is related to the period of the index variation Λ by

$$K = \frac{2\pi}{\Lambda} \tag{2-3}$$

The depth of modulation is typically much smaller than the average index of refraction (i.e. $n_0 >> n_1$). As an example, typical numbers for fiber Bragg gratings would be $n_0=1.46$ and $n_1=10^{-4}$.

With the index of refraction defined, it can now be used in the wave equation. The wave equation for light propagating along the x axis is given by

$$\frac{d^2}{dx^2}E(x)+(\frac{\omega}{c}n)^2E(x)=0, \qquad (2\text{-}4)$$

where ω is the angular frequency and c is the velocity of light in a vacuum. By assuming that $n_0 >> n_1$, and substituting $n(x)$ into the wave equation, the equation simplifies to

$$\frac{d^2}{dx^2}E(x)+\frac{\omega^2}{c^2}({n_0}^2+2n_0n_1\cos Kx)E(x)=0. \qquad (2\text{-}5)$$

This differential equation can be solved using coupled mode analysis. The electric field can be expressed in terms of normal modes of the unperturbed structure, where the expansion coefficients depend on x. In other words, the solution to Eq. (2-5) can be written as the sum of a forward traveling plane wave (A) and a reverse traveling plane wave (B),

$$E(x)=A(x)e^{-ikx}+B(x)e^{ikx}, \qquad (2\text{-}6)$$

where $\exp(-ikx)$ and $\exp(ikx)$ are the normal modes of the unperturbed structure.

The wavevector k is given by

$$k = \frac{2\pi n_0}{\lambda} = \frac{\omega}{c} n_0 . \tag{2-7}$$

If A(x) and B(x) are constant, Eq. (2-6) is the general solution to the unperturbed case. A(x) and B(x) were made functions of x because with a perturbation (i.e. $n_1 \neq 0$), the modes exp(-ikx) and exp(ikx) are no longer the normal modes of the whole structure.

Begin the analysis by plugging the solution, Eq. (2-6), into the wave equation to obtain

$$\begin{aligned} &A'' e^{-ikx} + B'' e^{ikx} - 2ikA' e^{-ikx} + 2ikB' e^{ikx} + \\ &2\frac{\omega^2}{c^2} n_0 n_1 (Ae^{-ikx} + Be^{ikx}) \cos(Kx) = 0, \end{aligned} \tag{2-8}$$

where a prime indicates a differentiation with respect to x.

This equation can be simplified further by assuming that the sinusoidal index variation is weak such that the variation of the amplitude is slow and satisfies the condition

$$|A''| << |kA'| \quad \text{and} \quad |B''| << |kB'|. \tag{2-9}$$

This condition is known as the parabolic approximation and is often used when perturbations are small. The simplified equation becomes

$$2ikA' e^{-ikx} - 2ikB' e^{ikx} = 2\frac{\omega^2}{c^2} n_0 n_1 \cos(Kx)(Ae^{-ikx} + Be^{ikx}) . \tag{2-10}$$

To further simplify, both sides of the equation can then be multiplied by exp(ikx). By averaging, rearranging, and the realization that the sinusoidal and exponential are only significant when $2k \approx K$, the simplified equations can be written as

$$A' = -i\frac{\omega n_1}{2c} B e^{i(2k-K)x}, \text{ and } \quad B' = i\frac{\omega n_1}{2c} A e^{-i(2k-K)x}. \quad (2\text{-}13)$$

The two differential equations can be further simplified by defining some constants. The first one is a coupling constant given by

$$\kappa = \frac{\omega n_1}{2c} = \frac{\pi n_1}{\lambda}, \quad (2\text{-}14)$$

and the second is a phase mismatch term given by

$$\Delta\beta = 2k - K. \quad (2\text{-}15)$$

The final coupled equations can be written as

$$\frac{d}{dx} A(x) = -i\kappa B(x) e^{i\Delta\beta x}, \text{ and } \quad \frac{d}{dx} B(x) = i\kappa A(x) e^{-i\Delta\beta x}. \quad (2\text{-}16)$$

The general solution for A(x) can be found by multiplying both sides of the first equation by exp($-i\Delta\beta x$) and then differentiating with respect to x. With some substitution and algebra, this method allows B(x) to be eliminated and forms a second order differential equation. The general solution then becomes

$$A(x) = [C_1 \cosh(sx) + C_2 \sinh(sx)] e^{i(\Delta\beta/2)x}, \quad (2\text{-}17)$$

where C_1 and C_2 are arbitrary constants and s is given by

$$s^2 = \kappa^2 - (\frac{\Delta\beta}{2})^2. \quad (2\text{-}18)$$

The term B(x) can be found by simply rearranging the first equation in (2-16) and is given by

$$B(x) = \frac{i}{\kappa} e^{-i\Delta\beta x} \frac{d}{dx} A.(x) . \qquad (2\text{-}19)$$

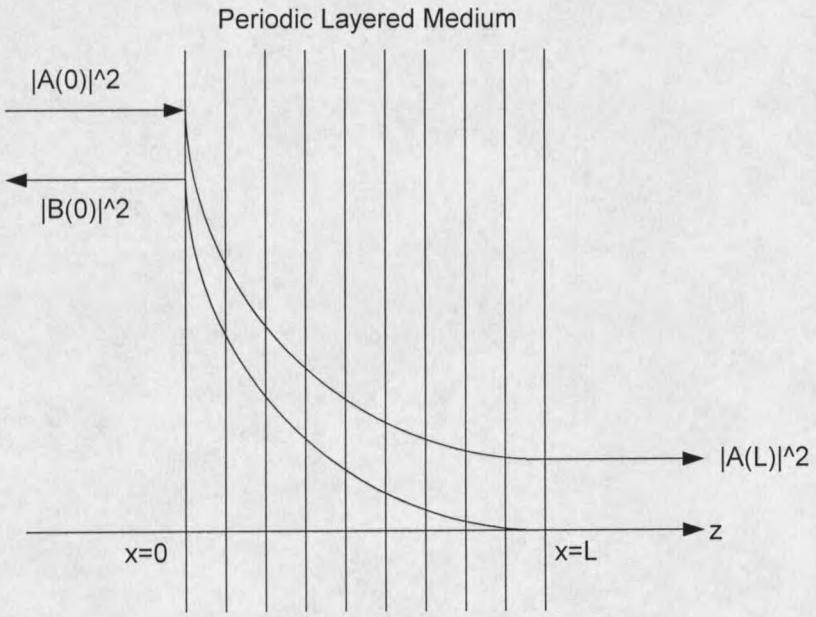

Figure 2-1: Mode powers of the incident mode (A(x)) and the reflected mode (B(x)) in a periodic layered medium when $\Delta\beta$=0.

With that complete, the reflection coefficient can now be found. Assuming the light is incident at x = 0, then the reflection coefficient can be written as

$$r = \frac{B(0)}{A(0)} . \qquad (2\text{-}20)$$

Notice in Figure 2-1 that the number of layers is assumed to be large enough that the amplitude of reflected light at the end of the structure, $x = L$, will be zero. This means that at some certain wavelength, all of the light will be reflected and none of it will reach the end of the structure. Using these boundary conditions, the equations for $A(x)$ and $B(x)$ can be written as

$$A(x) = \frac{s\cosh s(L-x) + i(\Delta\beta/2)\sinh s(L-x)}{s\cosh sL + i(\Delta\beta/2)\sinh sL} A(0)e^{i(\Delta\beta/2)x},$$

$$B(x) = \frac{-i\kappa\sinh s(L-x)}{s\cosh(sL) + i(\Delta\beta/2)\sinh sL} A(0)e^{-i(\Delta\beta/2)x}. \tag{2-21}$$

Plugging Eq. (2-21) into the reflection coefficient equation gives

$$r = \frac{-i\kappa\sinh(sL)}{s\cosh sL + i(\Delta\beta/2)\sinh sL}. \tag{2-22}$$

From here, the reflectance can be found by taking the absolute square of r. The equation for the reflectance is finally given by

$$R = |r|^2 = \frac{\kappa^2\sinh^2 sL}{s^2\cosh^2 sL + (\Delta\beta/2)^2\sinh^2 sL}. \tag{2-23}$$

The fractional power exchange into the reverse wave decreases as the value of $\Delta\beta$ increases. A complete power exchange into the reverse wave only becomes possible when the phase matching condition is satisfied at $\Delta\beta = 0$. Equation (2-23) then becomes

$$R = \tanh^2(\kappa L), \tag{2-24}$$

where there is a maximum power transfer only if $\kappa L >> 1$, so that $\tanh(\kappa L) \approx 1$.

The phase mismatch term is the basis of a very important equation for designing Bragg gratings. This term can be rewritten as

$$\Delta\beta = 2k - K = \frac{4\pi n_0}{\lambda_0} - \frac{2\pi}{\Lambda} \quad . \tag{2-25}$$

When the phase matching condition is satisfied, the two expressions in Eq. (2-25) must be equal. Setting the two sides equal and rearranging gives

$$\Lambda = \frac{\lambda_0}{2n_0}. \tag{2-26}$$

This equation gives the relationship between the pitch of a grating and the wavelength of light that will be reflected inside some medium.

Modeling

Mathcad. The equation for the reflectance can be used to model the reflectance versus wavelength of sinusoidal Bragg gratings. A program was written for this project in Mathcad (see Appendix A) to model the reflectance and to predict the performance of the crystal Bragg gratings.

The Mathcad program uses a slightly different equation than the one derived above. The equation that was just derived assumes the angle of incidence is zero, which simplifies the equation. The coupling coefficient and the phase mismatch term both depend on the angle of incidence. The equations change slightly to

$$\kappa(\theta_i) = \frac{\pi n_1}{\lambda \cos(\theta_i)}, \text{ and} \tag{2-27}$$

$$\Delta\beta(\theta_i) = \frac{4\pi \cos(\theta_i)}{\lambda} - \frac{2\pi}{\Lambda}, \tag{2-28}$$

where θ_i is the angle of incidence. The angle dependence causes the reflectance to shift to lower wavelengths with increasing angle.

The model was used to get an intuitive feel for the effects of changing various parameters. As the length of the crystal increases, there should be more reflected light at the Bragg wavelength because of the increase in the number of interfaces. An increase in the modulation depth should also increase the amount of reflected light because each interface has a larger index change.

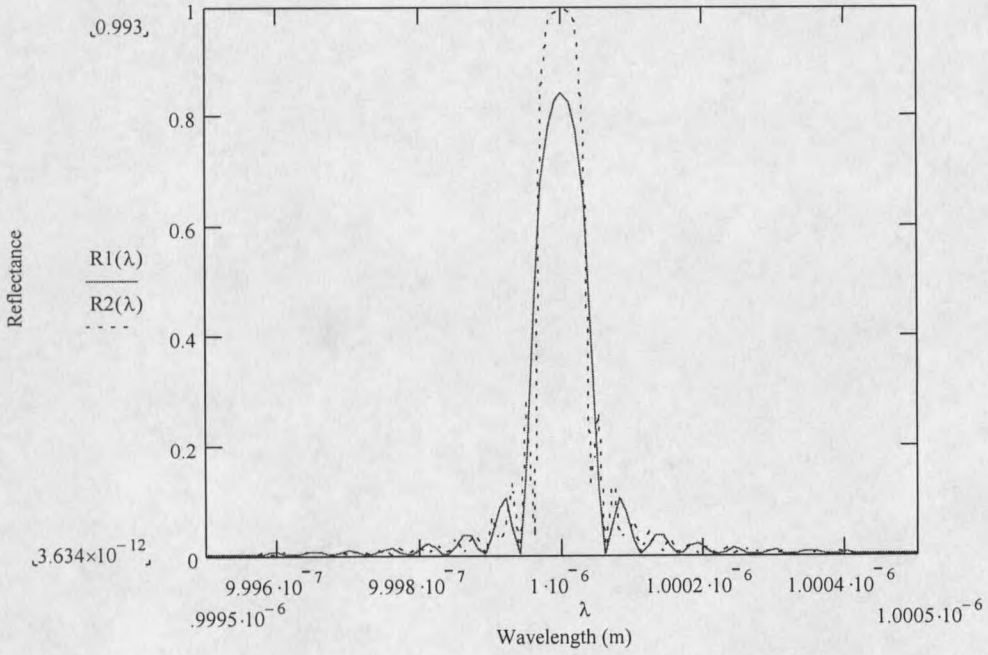

Figure 2-2: Reflectance from a 5mm and 10mm crystal.

The crystals were modeled under the assumption that the length of the crystal could vary between 5mm and 10mm. Due to the concentrations of the dopants inside the crystals, the modulation depth, Δn, was assumed to be

approximately $1\sim2*10^{-4}$. The exact pitch of the grating was inconsequential at this point. As shown in Figure 2-2, the reflectance changed from 0.84 to 1 using the assumed numbers where R1(λ) was the reflectance from a crystal 5mm long with $\Delta n=1*10^{-4}$ and R2(λ) was the reflectance from a 10mm crystal with $\Delta n =1*10^{-4}$. This showed that, at least theoretically, a crystal having either of the parameter sets, or anything in between, should have more than enough reflected signal to measure.

The length of the crystal is an easily changed parameter. The crystal could be fabricated with a bit more length. The depth of modulation is determined by the growth process, though this factor is not easily measured or controlled. Figure 2-3 shows another simulation with a 10mm crystal where $\Delta n=1*10^{-5}$. The reflectance has dropped considerably by changing the modulation depth. Changes in the grating growth process could generate smaller modulation depths.

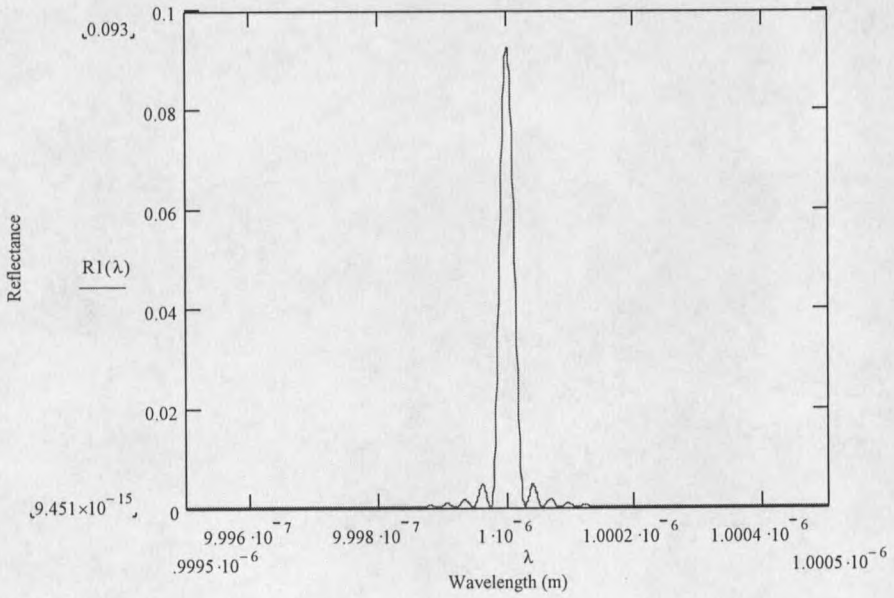

Figure 2-3: Reflectance from a 10mm crystal with a modulation depth of $1*10^{-5}$.